

Atmospheric Yield Functions and the Response to Secondary Particles of Neutron Monitors

J.M.Clem

Bartol Research Institute, University of Delaware, Newark, DE 19716, USA

Abstract

Angle dependent yield functions for different Neutron Monitor types are calculated using a simulation of cosmic ray air showers combined with a detection efficiency simulation for different secondary particle species. Results are shown for IGY and NM64 configurations using the standard $^{10}\text{BF}_3$ detectors and the new ^3He detectors to be used in the Spaceship Earth Project (Bieber and Evenson, 1995). The method of calculation is described in detail and the results are compared with measurements and previous calculations.

1 Introduction:

In order to understand the ground-based neutron monitor (NM) as a primary particle detector, a relationship between the count rate and primary flux must be established (Simpson 1948, Hatton 1971). Primary particles not rejected by the geomagnetic field enter the atmosphere and undergo multiple interactions resulting in showers of secondary particles which may reach ground level and be detected by a NM. Therefore a NM yield function of primary particles must incorporate the propagation of particles through the Earth's atmosphere and the detection response of a NM to secondary particles such as neutrons, protons, muons and pions.

2 Neutron Monitor Detection Efficiency:

To determine the neutron monitor (NM) detection response of secondary particles at ground level a simulation was performed using a 3-dimensional particle transport package entitled FLUKA (FLUcuating KAscades) (Fassó, et al., 1997) combined with programs written by the author to simulate the proportional tube and electronics response to energy deposition in the gas. The standard dimensions and composition of materials of a IGY and a NM-64 were used as input to the geometry (Hatton 1971). Initially a four meter diameter parallel beam of mono-energetic particles at a fixed angle fully illuminates the neutron monitor and is repeated for different incident beam angles, initial energy and particle species. Data are stored for every beam particle that produces a minimum value of energy deposited in any counter. These data are then used to generate a pulse height distribution which is integrated (with dead-time and pile-up effects) to determine the total number of counts per beam luminosity (number of beam particles/beam area).

Figure 1 displays the resulting detection efficiency of a NM-64 with $^{10}\text{BF}_3$ counters for 6 different particle species including neutrons, protons, positive and negative pions and muons for the vertical incident direction. Detector response is optimized to measure the hadronic component of ground level secondaries. The NM response from muons above 1 GeV is roughly 3.5 orders of magnitude below the hadrons. In this energy region, the primary mechanisms for muon induced counts is neutron production in photo-nuclear interactions and electromagnetic showers resulting in multiple ionization tracks in a counter. Below 1 GeV, stopping negative charge muons are captured by a lead nucleus into a mesic orbit and absorbed by the nucleus. The de-excitation of the nucleus occurs with the emission of neutrons which is reflected in the rise in detection efficiency with decreasing energy.

As expected, there is practically no difference in the response between neutrons and protons in the high energy region, while at lower energies the ionization energy loss of protons become significant, greatly reducing the probability of an interaction, which is reflected in the decreasing detection efficiency. Positive and negative charged pions produce almost identical responses at high energies while at lower energies negative pions undergo nuclear capture like negative muons, however the pion absorption time after capture is much less compensating the pions shorter decay-time as reflected in the rise in negative pion efficiency. It also should be noted that the pion inelastic cross sections are smaller than those of a nucleon in the high energy region

and therefore have a lower detection response since the NM vertical lead depth is only 80% of the nucleonic inelastic interaction pathlength.

Shown in figure 2 is the resulting detection efficiency for protons and neutrons in NM-64 and IGY compared with Hatton's calculation (1971) and NM-64 accelerator data (Shibata, et al., 1997). The dashed lines represents Hatton's calculation and solid lines represents this calculation. Unfortunately, the data lie in the only region where the calculations agree and the data are consistent with both calculations. Coincidentally, in this region lies the peak response for both NM-64 and IGY when ground-level spectra are considered. It is not clear why the two calculations differ outside this region.

Figure 3 displays the calculated detection response of an NM-64 for vertical incident neutron and proton beams. We show simulations for the traditional BP-28 detector employing $^{10}\text{BF}_3$ and for a detector using ^3He that we designed to have a similar response. The calculated ^3He NM-64 response is systematically slightly higher. Pyle, et al. (1999), reporting preliminary results from a recent latitude survey, suggest that the ^3He NM-64 response is roughly 5% higher than predicted by this calculation. Various small effects in the survey system not included in this simulation could contribute to this difference.

3 Yield Functions:

The propagation of primary particles through the Earth's atmosphere was calculated with the three dimensional Monte Carlo transport program FLUKA which is the same package that was used to calculate the neutron monitor (NM) detection efficiency. Primary particles are filtered through either a uniform or angle dependent effective rigidity cutoff (Clem et al., 1997, Lin et al., 1995) calculated for each geographical location, and the surviving particles are transported through the atmosphere. The simulated ground-level particle intensities, folded with the calculated NM detector response are then used to calculate a geographically dependent

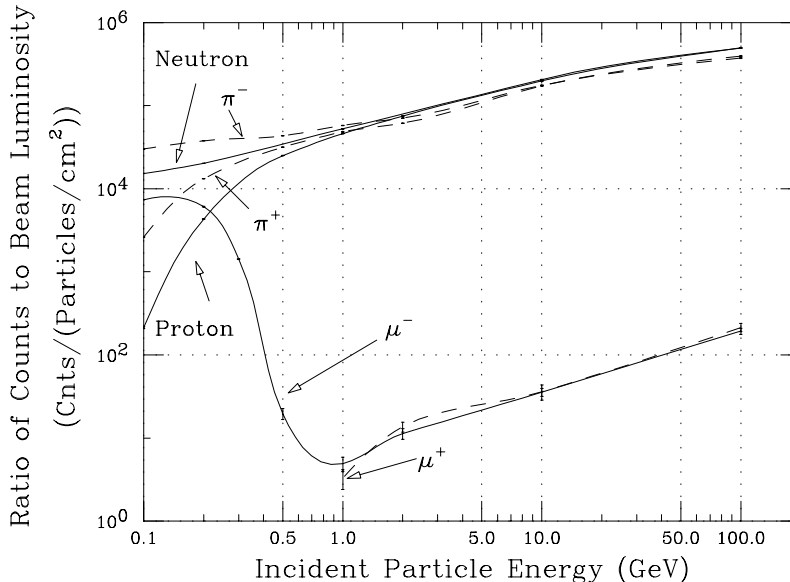


Figure 1: BP-28 NM64 calculated detection efficiency of secondary particles arriving in the vertical direction.

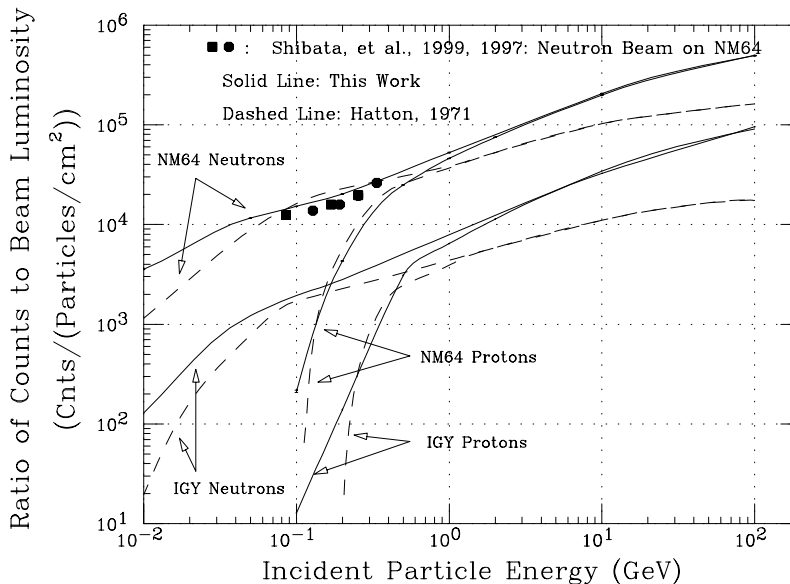


Figure 2: Comparison of NM detection efficiency with data and a previous calculation.

counting rate. The details of the simulation are described below.

Monoenergetic primary protons and alphas are generated at different fixed incident directions within the rigidity range of 1GV — 2000GV. Alpha particles are initially transported with a separate package called HEAVY (Engel 1992) to simulate fragmentation. This package interfaces with FLUKA to provide interaction starting points for each nucleon originating from a helium nucleus. The atmosphere is divided into sixty Earth-size (bottom boundary radius = 6378km) concentric spherical shells with differing radii and density to simulate the actual density profile (Gaisser 1990) with a vertical total 1033g/cm² column density for sea level. Above 500 meters the atmospheric composition (Zombeck 1982) is constant with a 23.3% O₂, 75.4% N₂ and 1.3% Argon distribution by mass while below 500 meters a varying addition of H₂ from 0.06% at sea-level to 0.01% at 500 meters is included to account for the abundance of water vapor. The outer air-space boundary is radially separated by 65 kilometers from the inner ground-air boundary. A single 1 cm² element on the air-space boundary is illuminated with primaries. This area element defines a solid angle element with respect to the center of the Earth which subtends a slightly smaller area element on the ground. Particle intensity at sea-level is determined by superimposing all elements on the bottom boundary. Due to rotational invariance this process is equivalent to illuminating the entire sky and recording the flux in a single element at ground level, but requires far less computer time.

To convert ground-level particle intensities to a NM counting rate one must weight each ground level particle by the NM detection efficiency, as described in the previous section. Therefore the NM yield function

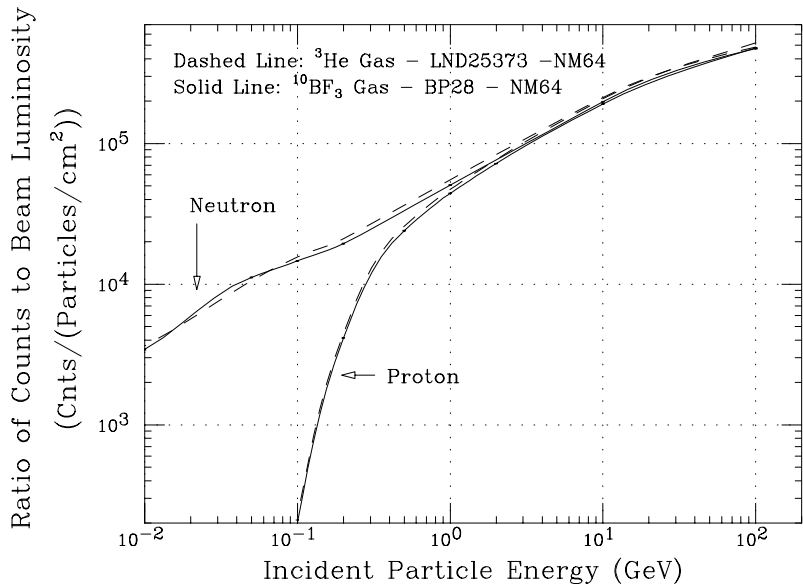


Figure 3: Calculated detection efficiency of ³He NM-64 and ¹⁰BF₃ NM-64 for protons and neutrons.

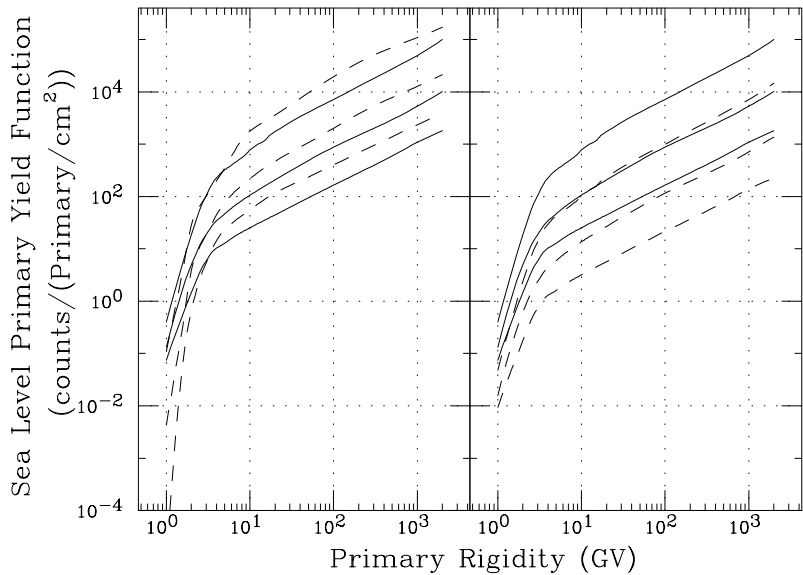


Figure 4: In the right frame, the yield function of an IGY (dashed lines) and NM64 (solid lines) from primary protons arriving at 0°, 45° and 60° incidence are shown. In the left frame, the yield function of NM64 from primary alphas (dashed lines) are also shown for same arriving incidence. The solid lines shown in both frames are the same.

of primary particles is the sum of ground level particles weighted by the NM detection efficiency divided by the primary particle beam density of fixed rigidity and incident angle. In other words, the yield function represents the NM detection efficiency of primary particles. Figure 4 displays the yield function calculation at sea level for 3 different conditions. The solid line in both left and right frames represents the NM-64 yield function from primary protons arriving at different fixed incident angles with respect to the zenith at the top of the atmosphere. The top curve represents vertical incident primaries with 0° , the middle curve represents the 45° incident direction and the bottom is 60° . The dashed lines in the left frame represents the NM-64 yield function for primary alpha particles while the dashed lines in the right frame represents the IGY yield function for primary protons. As expected, the smaller IGY results in a lower yield function, but having a similar shape. For the same high rigidity, one would expect alphas to have a higher yield due to having a larger total kinetic energy than protons, however at lower rigidities the higher ionization energy loss of alphas is more effective in preventing inelastic collisions than for protons, which is reflected in the cross-over in yields.

The NM response function can be determined by folding the primary proton and alpha cosmic ray spectra with the appropriate yield function. The counting rate for latitude surveys can then be calculated through integrating the resulting response functions over rigidity. These are compared to latitude survey observations in Clem et al. (1997, 1999). They show the simulation represents the data fairly well, however it produces a slope that is roughly 1% steeper than observations using primary spectra from Badhwar et al. (1997) and Seo et al. (1991) with proper solar modulation parameters.

4 Summary:

The simulated detection efficiency seems to be in agreement with published measurements, however the origin of the difference between this work and Hatton's calculation (1971) is not yet known. Even though more work is needed to determine the source of the discrepancies between the latitude survey calculation and observations, the current version of the simulation seems to perform fairly well considering the technique used, in which the fundamental nature of each component in a neutron monitor can be analyzed separately.

Acknowledgements

I want to thank John Bieber, Paul Evenson and Roger Pyle for their assistance in this project. This work was supported by NSF grants OPP-9528122, ATM-9616610, OPP-9724293, and OPP-9805780.

References

- Badhwar, G., 1997, Radiation Research, 148, S3-S10
- Bieber, J.W., et al., 1995, Proc. 24 ICRC (Rome), Vol 4, 1316
- Clem, J.M., et al., 1997, JGR, Vol. 102, No. A12, 26919
- Clem, J.M., et al., in preparation, 1999, Cosmic Rays and Earth, ISSI publication
- Engel, J., T.Gaisser, P. Lipari and T.Stanev, 1992, Phys. Rev. D46, 5013
- Fassò, A., et al., 1997, CERN Divisional report CERN/TIS-RP/97-05, 158
- Gaisser, T., 1990, Cosmic Rays and Particle Physics, Cambridge University Press
- Hatton, C.J., 1971, Progress in Elementary Particle and Cosmic Ray Physics, Vol. X, American Elsevier
- Lin, Z., et al., 1995 JGR, Vol 100, No. A12, 23543
- Pyle, R., et al., 1999, Proc. 26 ICRC (Salt Lake City), SH.3.6.26
- Seo, E., et al., 1991, ApJ 378, 763
- Shibata, S., et al., 1997, Proc. 25 ICRC (Durban), Vol 1., 45
- Simpson, J., 1948, Phys. Rev., 73, 1389
- Zombeck, M., 1982, Handbook of Space Astronomy and Astrophysics, Cambridge University Press